ISBN: 978-3-95450-233-2 ISSN: 2673-5504 doi:10.18429/JACoW-SRF2021-SUPFDV016

A LOW POWER TEST FACILITY FOR SRF THIN FILM TESTING WITH HIGH SAMPLE THROUGHPUT RATE

D. Seal[1,2] *, T. Sian[1,2], O.B. Malyshev[2,3], P. Goudket[2,3], R. Valizadeh[2,3], J. Conlon[2,3], G. Burt[1,2]
[1]Engineering Department, Lancaster University, Lancaster LA1 4YR, UK
[2]Cockcroft Institute, STFC Daresbury Laboratory, Daresbury, Warrington WA4 4AD, UK
[3]ASTeC, STFC Daresbury Laboratory, Daresbury, Warrington WA4 4AD, UK

Abstract

A low-power SRF test facility is being upgraded at Daresbury Laboratory as part of the superconducting thin film testing programme. The facility consists of a bulk niobium test cavity operating at 7.8 GHz, surrounded by RF chokes, and can be run with input RF powers up to 1 W. It is housed within a liquid helium free cryostat and is able to test thin film planar samples up to 100 mm in diameter with a thickness between 1 and 20 mm. The RF chokes allow the cavity to be physically and thermally isolated from the sample, thus reducing the need for complicated sample mounting, whilst minimising field leakage out of the cavity. This allows for a fast turnaround time of two to three days per sample. Initial tests using a newly designed sample holder have shown that an RF-DC compensation method can be used successfully to calculate the surface resistance of samples down to 4 K. Potential upgrades include a pick-up antenna for direct measurements of stored energy and the addition of a self-excited loop to mitigate the effects of microphonics. Details of this facility and preliminary results are described in this paper.

INTRODUCTION

The main aim for the thin film SRF programme at Daresbury Laboratory is to have a simple system able to measure samples under RF conditions with a quick turnaround time between tests. A vertical test facility able to achieve this is in the final stages of commissioning.

After commissioning of the system has been completed, it is expected that two to three samples can be fully characterised under RF conditions per week. This is made possible because of a simple sample mounting procedure that requires little time and effort to perform as it does not require welding.

The ultimate aim is to have the system running in tandem with both a magnetic field penetration facility [1] and a RRR facility [2] operating at Daresbury Laboratory. In doing so, a full picture can be built up of how well each sample performs under both RF and DC conditions. This can then be compared with deposition/preparation parameters used as well as results from surface analysis techniques in order to inform future full cavity depositions.

This paper reports on upgrades made to the test facility as well as RF testing and preliminary measurements of the surface resistance of a bulk niobium sample.

* daniel.seal@cockcroft.ac.uk

THE FACILITY

The facility consists of a bulk-niobium choked cavity as described in [3–5]. There are two versions of the cavity design available to use. Both consist of an identical cylindrical half cell, with one surrounded by two chokes and the other surrounded by three chokes. These are both able to test planar samples up to 100 mm in diameter with variable thicknesses between 1 and 20 mm. The resonant frequency of the cavities is 7.8 GHz. This frequency was chosen due to the requirement of chokes surrounding the half cell, thus limiting its size. This, along with to the maximum size of planar samples able to be manufactured, result in a higher resonant frequency compared with most other test facilities.

Planar samples are used because they are easy to deposit on and can be manufactured at low cost unlike full sized cavities. Preparation and deposition of thin film samples of niobium, as well as other superconducting compounds, by members of ASTeC are detailed in [6–8].

The choke cavity is housed in a two-stage LHe-free cryostat. This system is described fully in [5]. The system allows for a simple, fast sample changeover, justifying the decision to switch from using a previous LHe cryostat [4]. The facility contains a laminar air flow providing cleanliness to ISO 6 standard, though moving to a cleaner environment might be required in the future.

There have since been some modifications to this dry system. The main upgrade has been to the sample mounting system. The previous design was deemed to provide poor thermal control of the sample. In order to improve on this, the sample holder that mounts the sample to the system was redesigned. The new sample holder, made from OFHC copper is brazed at 160 °C with indium foil to the sample prior to installation in the cryostat. This is carried out in a separate facility, either under vacuum or in the presence of an inert gas, to ensure that there is minimal contamination of the sample. The high thermal conductivity of indium provides a strong thermal contact between the sample holder and sample allowing for more accurate temperature measurements and optimal thermal control. Since it is not possible to attach thermometers directly to the sample, two silicon diode thermometers are mounted to the sample holder. The sample holder also has two 10 Ω heaters attached as well as copper heat links connected to the cold head for cooling.

Another upgrade was made to improve the thermal isolation between the sample and cavity. To maintain a 1mm vacuum gap between the two, aluminium spacers were previously used. However, these spacers were later replaced

ISBN: 978-3-95450-233-2 ISSN: 2673-5504 doi:10.18429/JACoW-SRF2021-SUPFDV016

by G-10 material in order to achieve better thermal isolation. This is important when using an RF-DC compensation method, detailed in [9, 10], for measuring power dissipated on the sample. With the G-10 spacers, a temperature difference between the sample and cavity of 4 K was achieved compared with just 0.1 K with the aluminium spacers with no additional cooling on the sample.

The sample holder slides onto an aluminium sample plate and is mounted using G-10 studdings to ensure that the sample is aligned with the cavity. A schematic of the upgraded mounting system is shown in Fig. 1 with an image of this shown in Fig. 2.

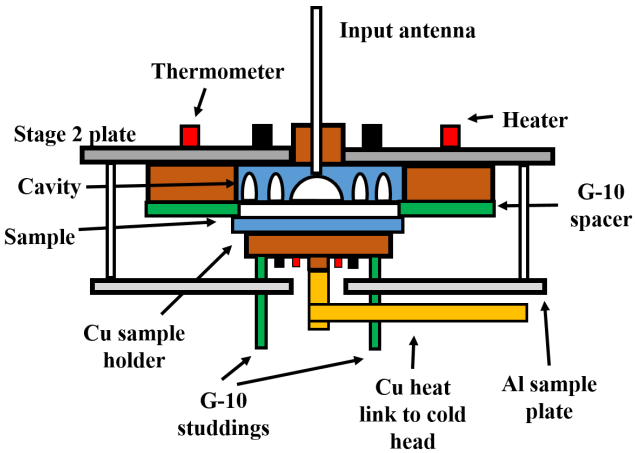

Figure 1: A schematic showing the mounting of the cavity and sample to the stage 2 plate of the cryostat.

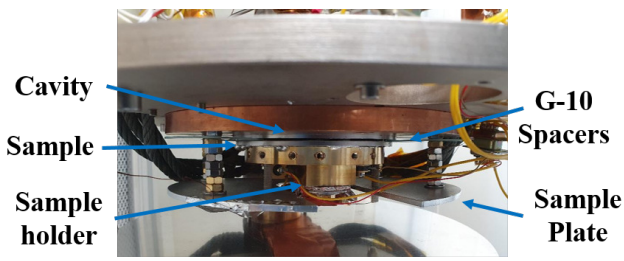

Figure 2: A view of the sample mounted under the cavity.

The third upgrade made had the aim of making more accurate thermometry measurements. To do this, one has to measure the power dissipated on the sample by the heaters. In order to do this accurately, the facility has had the addition of Multicomp Pro multimeters connected between the sample heaters and a Lakeshore temperature controller. An equivalent set up is in place for the heaters to connected to the cavity plate. These multimeters allow for a four wire measurement of current and voltage across the heaters connected to the sample holder, required for measurements of DC power across the heaters. It is important that the choke cavity temperature is kept constant using a separate Lakeshore controller connected to the cavity heaters in order to keep the Q factor of the cavity-sample system constant during the measurement.

The main advantage of the facility is the simplicity of changing samples. Assembling the cryostat, from opening up to replacing a sample and closing, takes only around 1 hour. It then takes around 2 hours to pump down to 10^{-3} mbar before the compressor is switched on to start cooling. The sample and cavity take around 12 hours to cool to a base temperature of approximately 4 K. Allowing one day for taking measurements means that completing a sample test can take just two days.

RF-DC COMPENSATION METHOD

The RF surface resistance of samples, R_S, is measured using a simple RF-DC compensation method, based on that used by the quadrupole resonator described in [9, 10]. This utilises the heaters connected to both the cavity and the sample which performs measurements at a fixed temperature with the RF on and off, hence removing calibration errors. The procedure is as follows:

1. Starting at an initial sample temperature, the temperature of interest of the sample, T_s, is set with the RF off. This is done using the temperature controller connected to the sample heaters, which supplies a current to them. Once T_s and heater power, P_{DC}, have both stabilised, a first measurement of heater power, $P_{DC,1}$, is made by measuring the current through the heaters and the voltage across them.

2. The RF power is switched on, which causes a momentary rise in sample temperature due to RF heating on the sample surface. The temperature controller then brings the temperature back down to the value previously set and the new value of DC power through the heaters is measured to be $P_{DC,2}$.

3. The RF power dissipated on the sample, P_{RF}, is equal to the difference in heater powers. I.e. $P_{RF} = P_{DC,1} - P_{DC,2}$.

4. Steps 2 and 3 can be repeated at a range of RF powers and hence a range of magnetic field strengths on the sample. Each time, a new value of $P_{DC,2}$ is measured.

An example of how T_s and P_{DC} vary over time is shown in Fig. 3 for a change of T_s from 4.0 to 4.2 K. T_s reaches equilibrium after just a few minutes, however it usually takes around 30 minutes for the heater power to stabilise. This is likely due to the low thermal conductivity of the niobium sample. P_{DC} and T_s take just a few minutes to stabilise when RF power, P_{cav}, is input into the cavity due to the fact that T_s remains constant, allowing for measurements to be taken at a range of RF powers. The small drop in P_{DC} as P_{cav} is increased from 0 indicates that only a small percentage of RF power is dissipated on the sample. The rest of the power is both dissipated on the sample and radiated through the sample-cavity gap.

P_{RF} is defined as

ISBN: 978-3-95450-233-2 ISSN: 2673-5504 doi:10.18429/JACoW-SRF2021-SUPFDV016

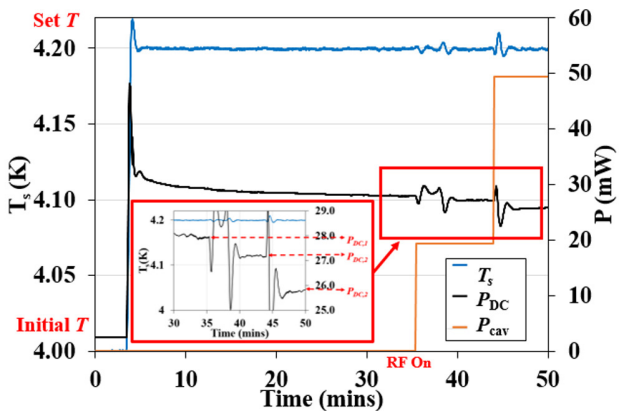

Figure 3: An example of how T_s and P_{DC} vary with time before and after RF power is switched on. Both P_{DC} and P_{cav} are plotted on the secondary axis. Two values of $P_{DC,2}$ are shown for two values of P_{cav}.

$$P_{RF} = \frac{1}{2\mu_0^2} R_S \int_{Sample} |\boldsymbol{B}|^2 dS, \quad (1)$$

where μ_0^2 is the vacuum permeability, $\boldsymbol{B}$ is the magnetic field strength and it is assumed that R_S is constant over the sample surface.

Following steps 1 to 3 allows for direct measurements of R_S from a rearrangement of Eq. (1):

$$R_S = \frac{2\mu_0^2 P_{RF}}{\int_{Sample} |\boldsymbol{B}|^2 dS}. \quad (2)$$

The surface integral in Eq. (2) cannot be determined experimentally, therefore a constant has to be defined in order to calculate R_S. This constant, c, is defined as:

$$c = \frac{2B_{s,pk}^2}{\int_{Sample} |\boldsymbol{B}|^2 dS} = \frac{B_{s,pk,CST}^2 R_{S,CST}}{\mu_0^2 P_{s,CST}}. \quad (3)$$

where $B_{s,pk}$ is the peak magnetic field on the sample surface given by

$$B_{s,pk} = B_{s,pk,CST} \times \sqrt{U}, \quad (4)$$

and U is the stored energy in the cavity.

In Eq. (3), $B_{s,pk,CST}$, $P_{s,CST}$ and $R_{s,CST}$ are values of the magnetic field, power dissipated on the sample and surface resistance calculated using CST Studio Suite [11] normalised for a stored energy of 1 J. For the choke cavity system, $c = 2.63 \times 10^3$ m^{-2}.

Substituting the constant into Eq. (2) gives an equation that can be used to calculate R_S:

$$R_S = \frac{c\mu_0^2 P_{RF}}{B_{s,pk}^2}. \quad (5)$$

Therefore, R_S measurements simply require being able to measure heater power and stored energy.

RF TESTS

Tests with this system continue to be made with reflection measurements via a single input coupler connected to a vector network analyser (VNA).

Prior to making the first R_S measurements of a bulk niobium sample using RF-DC compensation, it was important to quantify the level of microphonics in the system. It had previously been noted that moving from a LHe system to a Gifford-McMahon cryocooler increased the level of microphonics due to its mechanical motion causing vibrations of the input coupler [5]. This leads to excitations of mechanical modes within the system, which can couple with the resonant frequency of the cavity and create unwanted noise. The main downside of this is when measuring narrower bandwidths at the lower end of the temperature range leading to higher uncertainties in measurements of Q and P_{cav}.

To quantify the level of microphonics, the VNA was firstly set to a zero span frequency at the resonant frequency, f_0, and fluctuations in the S_{11} phase were measured over a period of time. The phase of the reflected signal, θ, is given by [12]:

$$\theta = -\arctan\left(\frac{2\beta Q_0 \delta}{\beta^2 - 1 - (Q_0\delta)^2}\right), \quad (6)$$

where β is the coupling factor and Q_0 is the intrinsic quality factor. The normalised frequency shift, δ, is given by

$$\delta = \frac{f}{f_0} - \frac{f_0}{f} \simeq \frac{2\Delta f}{f_0}, \quad (7)$$

where f is a frequency point and Δf is the frequency shift of the microphonics.

The phase shifts measured by the VNA were converted to a normalised frequency shift using Eq. (6). The maximum normalised frequency shift was approximately 1.5×10^{-5} which corresponds to $\Delta f \simeq 60$ kHz with a period of 1 s as shown in Fig. 4. This is around five times the expected bandwidth at low temperatures, indicating that the periodic motion of the cryocooler causes significant vibrations in the long input coupler.

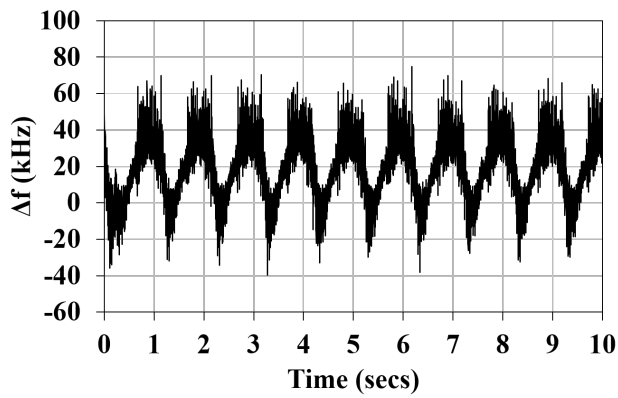

Figure 4: Measurements of Δf over a sweep time of 10 seconds.

Despite previous attempts to damp the microphonics [5], the level is still too high to make accurate measurements

ISBN: 978-3-95450-233-2 ISSN: 2673-5504 doi:10.18429/JACoW-SRF2021-SUPFDV016

with the single coupler in the matched state. Instead, all measurements have been taken with with the coupler overcoupled to widen the bandwidth above 60 kHz to keep the cavity on resonance. However, in doing so, more power leaks out of the coupler and less goes into the cavity. This therefore limits the strength of $B_{s,pk}$.

With the VNA limited to a maximum output power of 2.5 mW at 7.8 GHz, the addition of an amplifier was required to compensate for an overcoupled input coupler. The amplifier was connected in conjunction with attenuators allowing for a maximum input power into the cavity of 1 W (due to lab radiation limits). A directional coupler was used to direct the reflected signal from the cavity into the second port of the VNA due to the amplifier being unidirectional. This system can be adjusted to provide more input power if needed.

The amplifier system can also accommodate a second coupler acting as a pickup. The pickup can be used to make measurements of the transmitted power in the system, leading to direct measurements of U. This leads to more accurate measurements of $B_{s,pk}$ calculated using Eq. (4) due to the removal of errors made when measuring cable losses from reflection measurements with a single coupler. A second coupler can also be used with a self-excited loop allowing the cavity to be fixed on resonance with measurements run in matched conditions whilst mitigating the effects of vibrations in the system. Doing this would also allow for measurements to be made at higher $B_{s,pk}$.

PRELIMINARY RESULTS AND DISCUSSION

The main aim of the preliminary tests was to ensure that the RF-DC compensation method could be successfully used with this system to measure R_S of planar sample discs. To demonstrate this, measurements of R_S of a bulk niobium sample were made both as a function of T_s at constant $B_{s,pk}$, and as a function of $B_{s,pk}$ at constant T_s.

So far, the minimum sample and cavity temperatures measured was 3.9 K. The lowest sample temperature measured was 4.1 K to ensure that there was sufficient cooling power available to reduce the sample back to its equilibrium temperature after RF power is turned on. The measurements of R_S against $1/T_s$ are shown in Fig. 5 for a constant $B_{s,pk}$ = 0.55 mT.

At lower temperatures it is clear that R_S is higher than R_{BCS}. The residual resistance of the sample is approximately 17 μΩ, although it should be noted that the bulk Nb sample used for testing did not have any surface treatment or HPR. The results also shows a steep increase in R_S at $8 \leq T_s \leq 9$ K, below the expected T_C = 9.2 K for niobium. Also plotted is the theoretical BCS resistance, R_{BCS}, over the same temperature range at a resonant frequency of 7.8 GHz. This was calculated by the widely used SRIMP programme based on the original code by Halbritter [13].

Measurements of R_S against $B_{s,pk}$ for constant T_s were also made. These results show a slight dependence of R_S

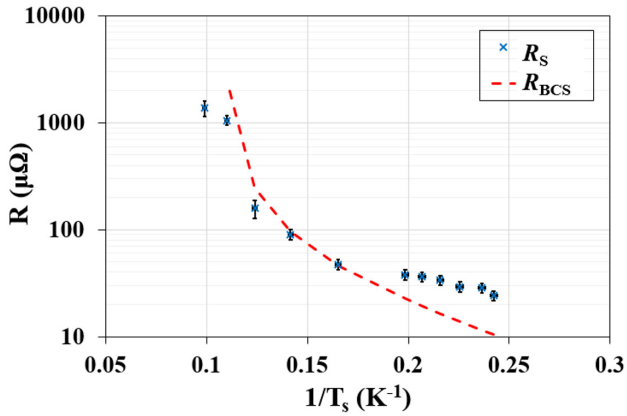

Figure 5: R_S and R_{BCS} vs $1/T_s$ with $B_{s,pk}$ = 0.55 mT.

on $B_{s,pk}$. Examples of this dependence are shown shown in Fig. 6 at T_s = 4.1 K and Fig. 7 at T_s = 4.4 K. The plots also show the measurements of $P_{DC,1}$ and $P_{DC,2}$. The difference between the two shows that the maximum P_{RF} = 1.8 mW at 4.1 K and P_{RF} = 2.2 mW at 4.4 K. Since $P_{DC,2}$ does not reach 0 mW in both cases, this indicates that the limitation with $B_{s,pk}$ = 0.55 mT is due to reaching the limit of P_{cav}. Mitigating the microphonics with a self-excited loop will allow the coupler to be in the matched state, allowing for more RF power input into the cavity resulting in higher $B_{s,pk}$.

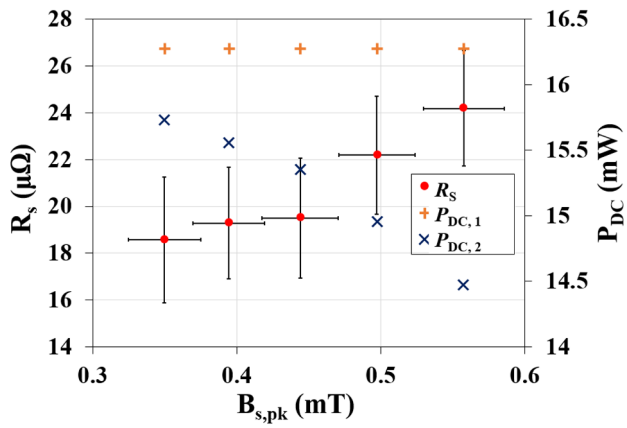

Figure 6: R_S vs $B_{s,pk}$ at T_s = 4.1 K.

The preliminary results for a bulk niobium sample show that this system can be used successfully to calculate R_S of samples via the RF-DC compensation method. Currently, one of the main contributors to the uncertainty in each measurement is how U is calculated. Just using a single antenna creates uncertainty in the value of P_{cav}, mainly due to cable losses. A second antenna acting as a pickup would enable direct measurements of U from the transmitted power, thus eliminating errors created from measuring cable loss factors.

ISBN: 978-3-95450-233-2 ISSN: 2673-5504 doi:10.18429/JACoW-SRF2021-SUPFDV016

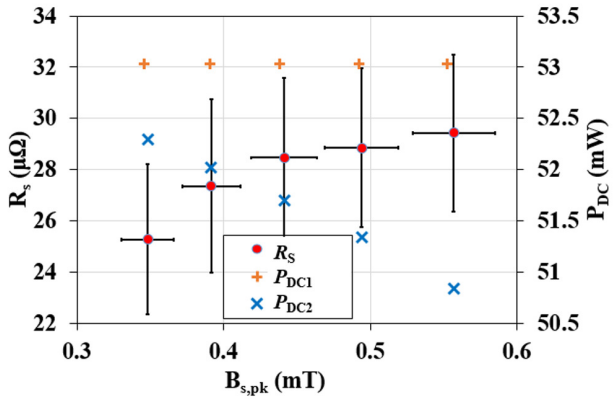

Figure 7: R_S vs $B_{s,pk}$ at T_s = 4.4 K.

CONCLUSIONS AND FUTURE UPGRADES

Measurements of R_S of a bulk niobium sample have been made for the first time using the RF-DC compensation method. These results successfully show that this method can be used for this system to test additional samples. Results show that measurements can currently be made down to T_s = 4.1 K and $B_{s,pk} \leq 0.55$ mT. The main advantage of this system is the ease of replacing and mounting a new sample. This means that two to three samples can be tested per week.

The main future upgrade will be the addition of a second coupler as a pickup that would allow for measurements of the transmitted power through the cavity, providing direct measurements of the stored energy in the cavity. This would remove any of the current uncertainties from measuring the stored energy from the reflected signal with a single input coupler. A second antenna would also allow for the possibility of adding a self-excited loop which would also allow for higher magnetic fields to be reached and a removal of the effects of microphonics.

With this system operational, it is ready to use for measuring thin film samples at a rate of two to three samples per week.

ACKNOWLEDGEMENTS

The authors wish to acknowledge support received by members of ASTeC, namely A. May, S. Hitchen, K. Dumbell, D. Turner and L. Smith. We also wish to acknowledge work carried out by staff in the Engineering Technology Centre at Daresbury Laboratory. D. Seal would like to thank UKRI for his PhD funding and T. Sian for his STFC/Cockcroft Institute grant.

REFERENCES

[1] D. Turner *et al.*, "A Facility for the Magnetic Characterisation of Planar Thin Film Structures," in *Proc. SRF 2021, virtual conference*, Jun-Jul 2021.

[2] O. Malyshev *et al.*, "Design, Assembly and Commissioning of a New Cryogenic Facility for Complex Superconducting Thin Film Testing," in *Proc. IPAC 2018, Vancouver, BC, Canada*, pp. 3859–3861, Apr-May 2018.

[3] L. Gurran *et al.*, "Superconducting Thin Film Test Cavity Commissioning," in *Proc. SRF 2015, Whistler, BC, Canada*, pp. 731–734, Sept 2015.

[4] P. Goudket *et al.*, "First Full Cryogenic Test of the SRF Thin Film Test Cavity," in *Proc. SRF 2017, Lanzhou, China*, pp. 644–646, Jul 2017.

[5] O. Malyshev *et al.*, "The SRF Thin Film Test Facility in LHe-Free Cryostat," in *Proc. SRF 2019, Dresden, Germany*, pp. 612–614, Jun-Jul 2019.

[6] R. Valizadeh *et al.*, "PVD deposition of Nb_3Sn Thin Film on Copper Substrate from an Alloy Nb_3Sn Target," in *Proc. IPAC 2018, Melbourne, Australia*, p. 2818, Jun-Jul 2018.

[7] R. Valizadeh *et al.*, "Synthesis of Nb and Alternative Superconducting Film to Nb for SRF Cavity as Single Layer," in *Proc. SRF 2021, virtual conference*, Jun-Jul 2021.

[8] F. Lockwood Estrin *et al.*, "Using HiPIMS to Deposit V_3Si Superconducting Thin Films," in *Proc. SRF 2021, virtual conference*, Jun-Jul 2021.

[9] T. Junginger, "Investigations of the Surface Resistance of Superconducting Materials," Jun 2012. Presented 25 Jul 2012.

[10] S. Keckert, "Optimizing a Calorimetry Chamber for the RF Characterization of Superconductors," Jul 2015.

[11] "CST Studio Suite." https://www.3ds.com/products-services/simulia/products/cst-studio-suite/.

[12] A. Mostacci, "Notes of Measurement Methodology of some RF Parameters," pp. 1–8, 2014.

[13] J. Halbritter, "Fortran-program for the computation of the surface impedance of superconductors.," 1970.